Supporting Information

A hybrid energy storage device: combination of zinc-ion supercapacitor and zinc-air battery in mild electrolyte

Guoqiang Sun,[a] Yukun Xiao,[a] Bing Lu,[a] Xuting Jin,[a] Hongsheng Yang,[a] Chunlong Dai,[a] Xinqun Zhang,[a] Yang Zhao,*[a] and Liangti Qu*[abc]

[a]Key Laboratory of Photoelectronic/Electrophotonic Conversion Materials, Key Laboratory of Cluster Science, Ministry of Education of China, School of Chemistry, Beijing Institute of Technology, Beijing 100081, P. R. China. E-mail: yzhao@bit.edu.cn; lqu@bit.edu.cn

[b]Key Laboratory for Advanced Materials Processing Technology, Ministry of Education of P. R. China; State Key Laboratory of Tribology, Department of Mechanical Engineering, Tsinghua University, Beijing 100084, P. R. China

[c]Department of Chemistry, Tsinghua University, Beijing 100081, P. R. China

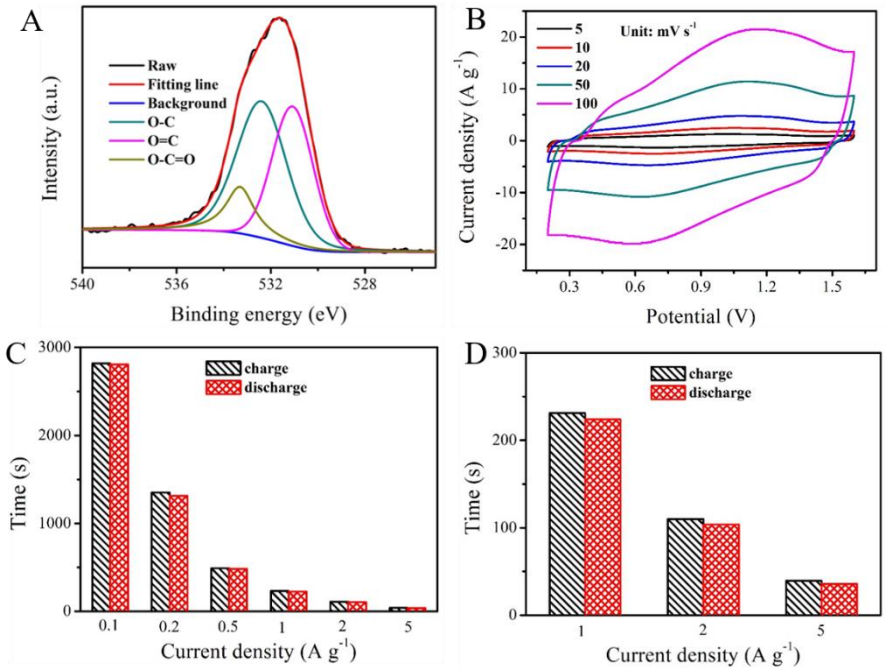

Figure S1. (A) High resolution XPS spectra of the O 1s peak of the RG-R. (B) CV curves of the ZISC in coin type. (C, D) Charge and discharge time at different current densities.

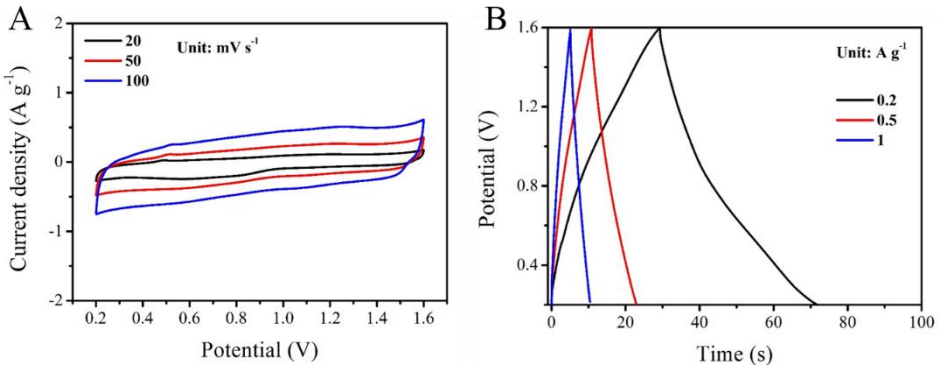

Figure S2. (A) CV and (B) GCD curves of the device constructed with AB and PVDF composite.

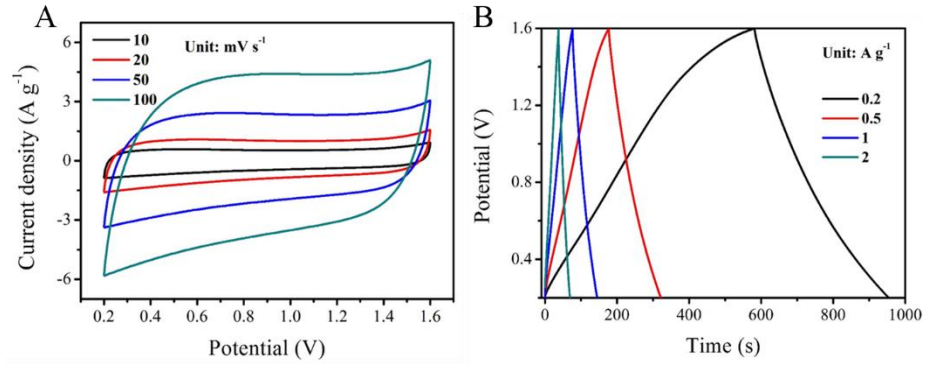

Figure S3. (A) CV and (B) GCD curves of the symmetric supercapacitor constructed with RG-R.

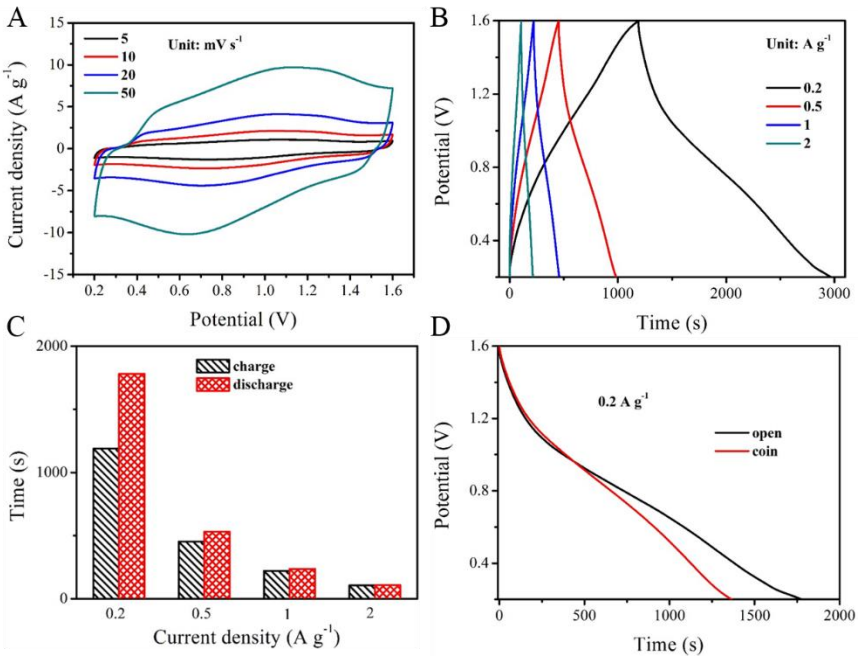

Figure S4. Electrochemical performance of the ZISC in air constructed with RG-F. (A) CV and (B) GCD curves. (C) Charge and discharge time at different current densities. (D) Discharge curves of the ZISC in air and coin type at a current density of 0.2 A g^{-1}.

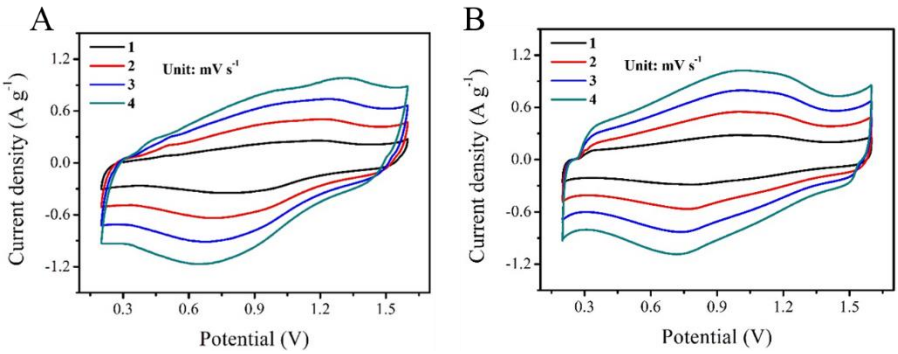

Figure S5. CV curves of the ZISC in (A) air and (B) coin type at different scan rates.

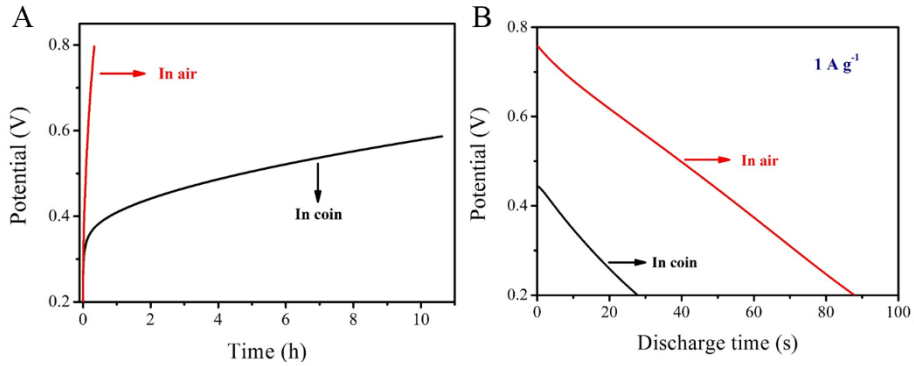

Figure S6. (A) The potential-time curves of ZISC in air and coin type. (B) The discharge curves in air and coin type.

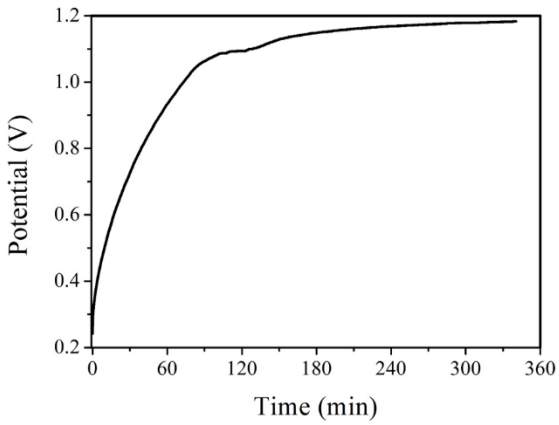

Figure S7. The potential-time curve of the ZISC with a standing time of 360 min.

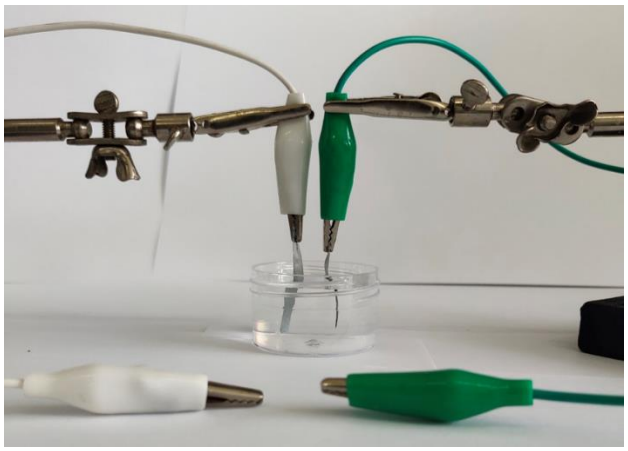

Figure S8. The photo of the ZISC in air atmosphere.

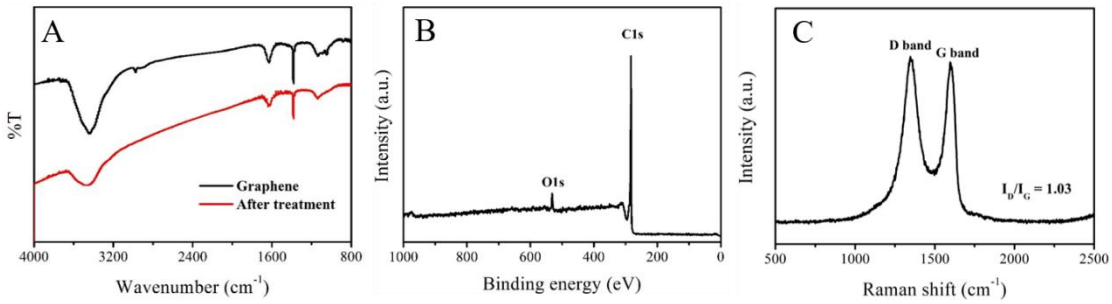

Figure S9. (A) FT-IR spectra, (B) XPS survey and (C) Raman spectra of RG-R1000.

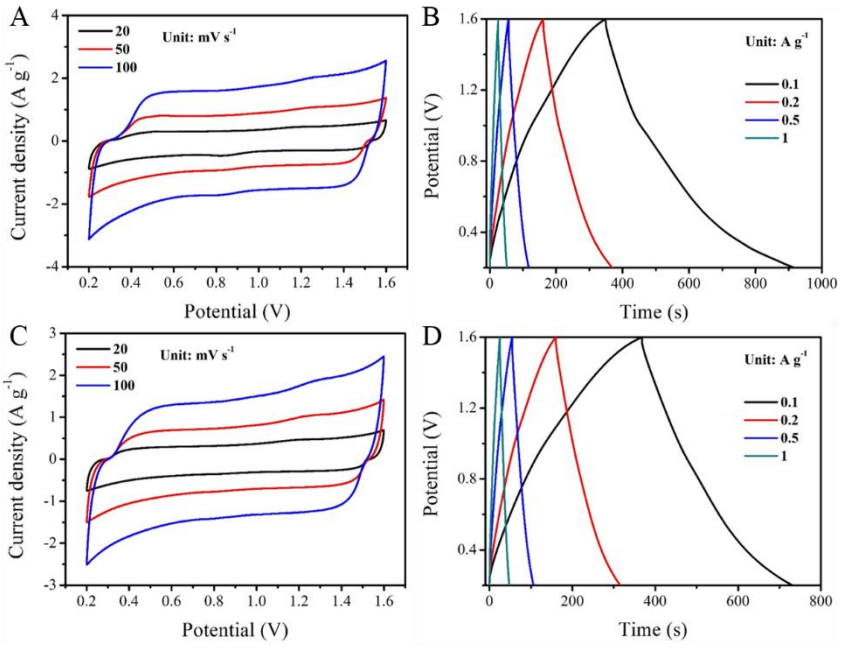

Figure S10. (A) CV and (B) GCD curves of ZISC constructed with RG-R1000 in air atmosphere. (C) CV and (D) GCD curves of ZISC constructed with RG-R1000 in coin type.

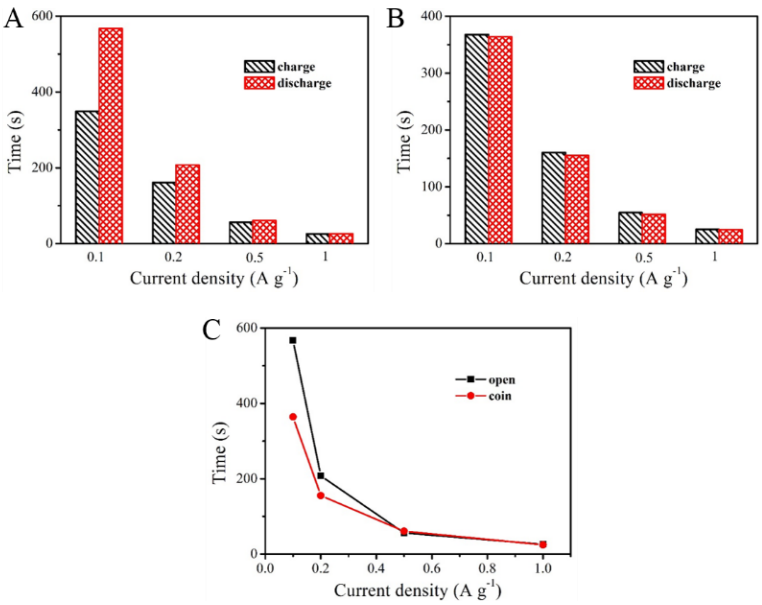

Figure S11. Charge and discharge time of ZISC constructed with RG-R1000 in (A) air atmosphere and (B) coin type. (C) Comparison of discharge time of the ZISC in air and coin type at different current densities.

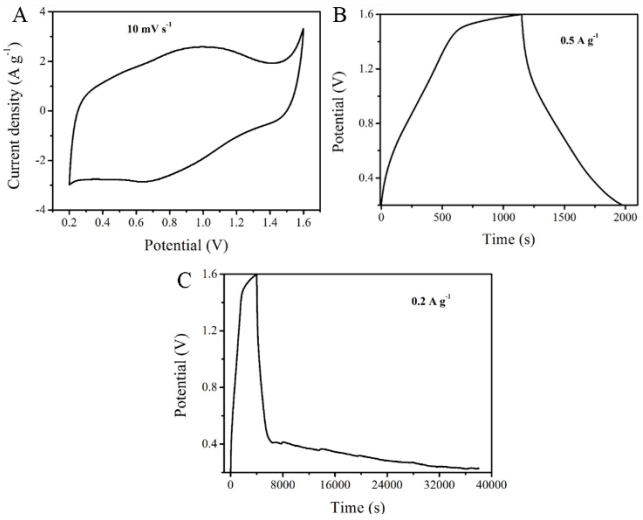

Figure S12. (A) CV curve of the ZISC with alkaline electrolyte at a scan rate of 10 mV s^{-1}. GCD curves of the ZISC at current density of (B) 0.5 A g^{-1} and (C) 0.2 A g^{-1}.

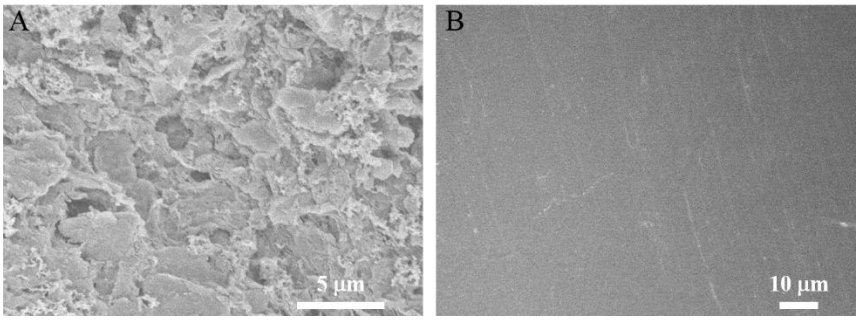

Figure S13. The SEM images of pristine (A) cathode and (B) anode.

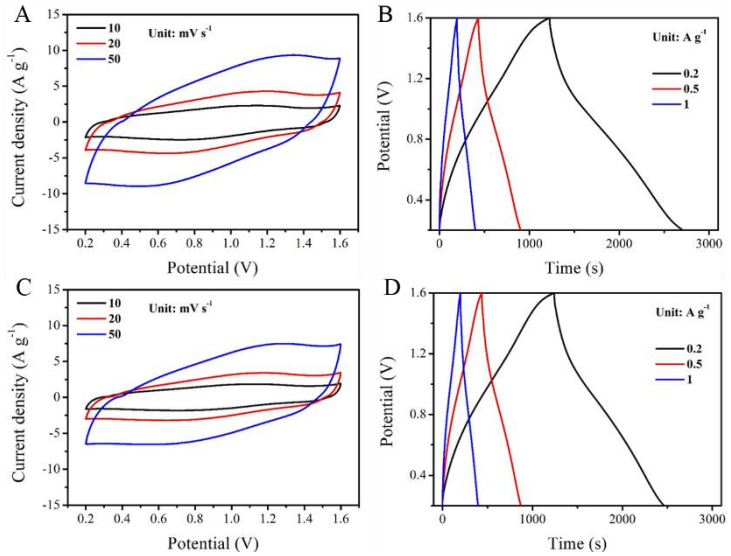

Figure S14. (A) CV and (B) GCD curves of ZISC constructed with RG-R ($Zn(AC)_2$ as electrolyte) in air atmosphere. (C) CV and (D) GCD curves of ZISC constructed with RG-R ($Zn(AC)_2$ as electrolyte) in coin type.

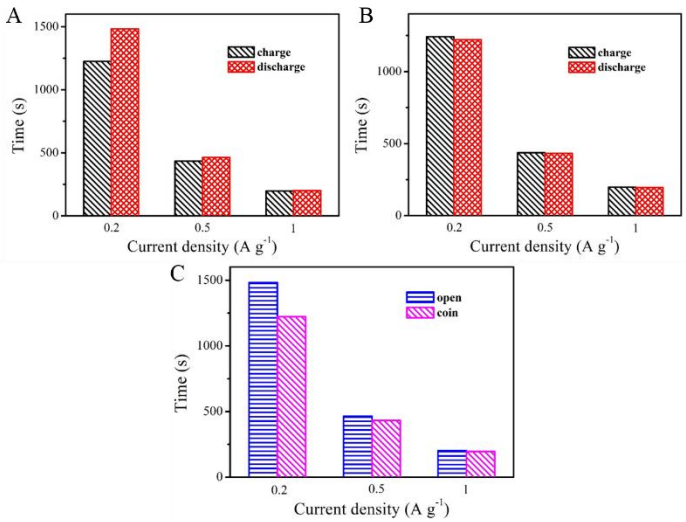

Figure S15. Charge and discharge time of ZISC constructed with RG-R ($Zn(AC)_2$ as electrolyte) in (A) air atmosphere and (B) coin type. (C) Comparison of discharge time of the ZISC in air and coin type at different current densities.

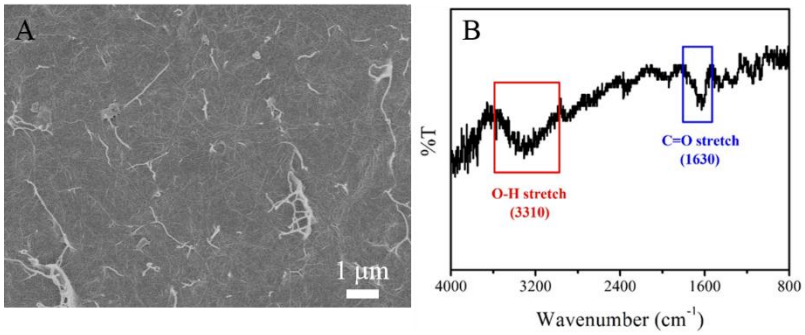

Figure S16. (A) SEM image and (B) FT-IR spectra of carbon nanotube paper.

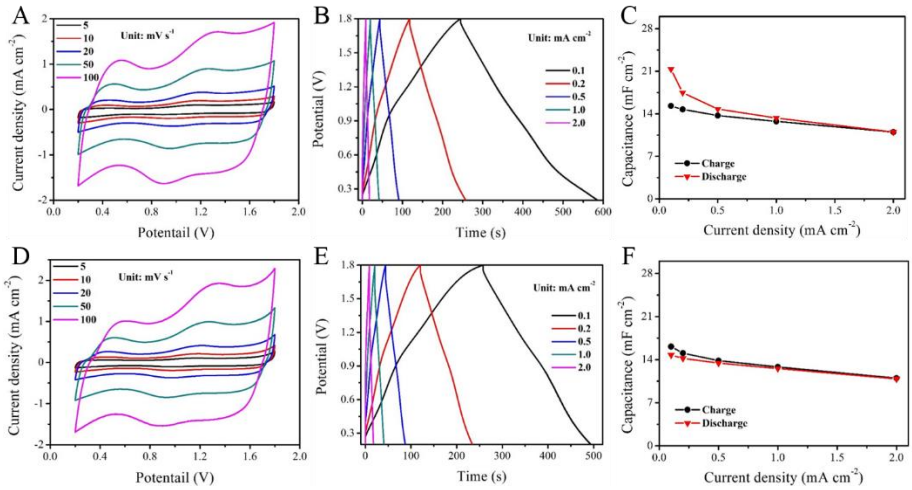

Figure S17. (A) CV and (B) GCD curves of ZISC constructed with carbon nanotube paper (1 M ZnSO4 as electrolyte) in air atmosphere. (C) Charge and discharge capacitance of the ZISC in air at different current densities. (C) CV and (D) GCD curves of ZISC constructed with carbon nanotube paper (1 M ZnSO4 as electrolyte) in coin type. (C) Charge and discharge capacitance of the ZISC in coin type at different current densities.

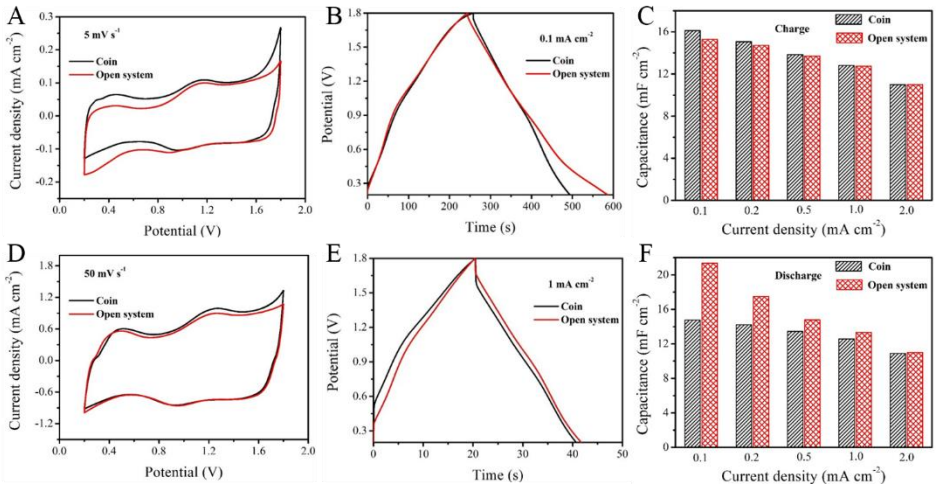

Figure S18. CV curves of the ZISC constructed with carbon nanotube paper in air and coin type at a scan rate of (A) 5 mV s^{-1} and (C) 50 mV s^{-1}. GCD curves of the ZISC constructed with carbon nanotube paper in air and coin type at a current density of (B) 0.1 mA cm^{-2} and (D) 1 mA cm^{-2}. Comparison of the (C) charge and (F) discharge time of the ZISC in air and coin type at different current densities.

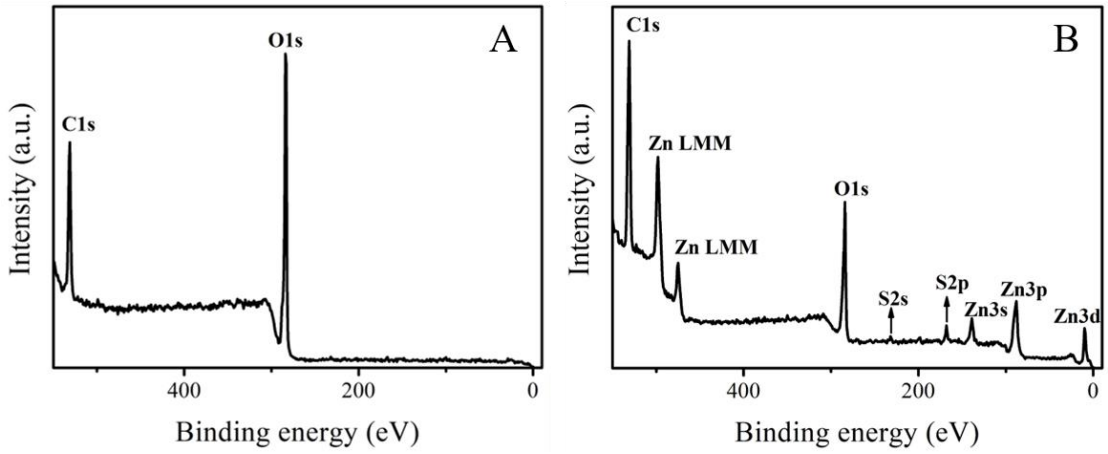

Figure S19. XPS spectra of carbon nanotube (A) before and (B) after treatment with $ZnSO_4$ electrolyte.

Table S1. Electrochemical properties of ZISC reported in literature and in this work.

Cathode	Operating voltage (V)	Energy density (Wh Kg^{-1})	Reference
Activated carbon	0-1.8	52.7	1
Hollow carbon spheres	0.2-1.8	59.7	2
Activated carbon	0.2-1.8	84	3
Graphite	0.5-1.8	53	4
Activated carbon	0-2	34.6	5
B/N co-doped porous Carbon	0.2-1.8	86.6	6
RuO_2	0.4-1.6	82	7
Graphene	**0.2-1.6**	**100.9**	**This work**

Table S2. Comparison of potential and discharge time of the ZISC with different standing time.

Standing time (min)	10	20	30	60	120	360	3
Potential (V)	0.652	0.755	0.840	1.029	1.098	1.116	0.795
Discharge time (s)	67	87.8	107	157.8	178	185.7	96.6

Table S3. The discharge time of the ZISC at different current densities after self-charging to 0.8 V.

Potential (V)	0.8	0.8	0.8
Current density (A g^{-1})	0.2	0.5	1
Discharge time (s)	718	217.9	94

References

(1) Wang, H.; Wang, M.; Tang, Y. B. A Novel Zinc-Ion Hybrid Supercapacitor for Long-Life and Low-Cost Energy Storage Applications. *Energy Storage Mater.* **2018**, *13*, 1-7.

(2) Chen, S. H.; Ma, L. T.; Zhang, K.; Kamruzzaman, M.; Zhi, C. Y.; Zapien, J. A. A Flexible Solid-State Zinc Ion Hybrid Supercapacitor Based on Co-polymer Derived Hollow Carbon Spheres. *J. Mater. Chem. A* **2019**, *7*, 7784-7790.

(3) Dong, L. B.; Ma, X. P.; Li, Y.; Zhao, L.; Liu, W. B.; Cheng, J. Y.; Xu, C. J.; Li, B. H.; Yang, Q. H.; Kang, F. Y. Extremely Safe, High-Rate and Ultralong-Life Zinc-Ion Hybrid Supercapacitors. *Energy Storage Mater.* **2018**, *13*, 96-102.

(4) Liu, Z.; Li, G. Z.; Cui, T.; Borodin, A.; Kuhl, C.; Endres, F. A Battery-Supercapacitor Hybrid Device Composed of Metallic Zinc, a Biodegradable Ionic Liquid Electrolyte and Graphite. *J. Solid State Electrochem.* **2018**, *22*, 91-101.

(5) Ma, X. P.; Wang, J. J.; Wang, X. L.; Zhao, L.; Xu, C. J. Aqueous V_2O_5/Activated Carbon Zinc-Ion Hybrid Capacitors with High Energy Density and Excellent Cycling Stability. *J. Mater. Sci-Mater. El.* **2019**, *30*, 5478-5486.

(6) Lu, Y. Y.; Li, Z. W.; Bai, Z. Y.; Mi, H. Y.; Ji, C. C.; Pang, H.; Yu, C.; Qiu, J. S. High Energy-Power Zn-ion Hybrid Supercapacitors Enabled by Layered B/N Co-doped Carbon Cathode. *Nano Energy* **2019**, *66*, 104132.

(7) Dong, L. B.; Yang, W.; Yang, W.; Wang, C. J.; Li, Y.; Xu, C. J.; Wang, S. W.; He, F. R.; Kang, F. Y.; Wang, G. X. High-Power and Ultralong-Life Aqueous Zinc-Ion Hybrid Capacitors Based on Pseudocapacitive Charge Storage. *Nano-Micro Lett.* **2019**, *11*, 94.